The 2013 World Congress on
Advances in Structural Engineering and Mechanics (ASEM13)
Jeju, Korea, September 8-12, 2013

Heat transfer analysis of hybrid stainless-carbon steel beam-column joints

Ali Razzazzadeh[1)], *Zhong Tao[2)] and Tian-Yi Song[3)]

[1), 2), 3)] *Institute for Infrastructure Engineering, University of Western Sydney, Penrith, NSW 2751, Australia*
[2)] z.tao@uws.edu.au

ABSTRACT

A finite element (FE) model is established to investigate the temperature field of hybrid stainless-carbon steel beam-column composite joints under the ISO 834 fire including a cooling phase. Two types of joints, including concrete filled carbon steel tubular column to steel beam joints and concrete filled stainless steel tubular column to steel beam joints are simulated. Based on the FE modelling, the temperature development of the composite joints in the heating and cooling fire stages is analysed and discussed.

Keywords: concrete filled steel tube (CFST); stainless steel; hybrid structure; joint; temperature field; fire

1. INTRODUCTION

Concrete filled steel tubular (CFST) columns have been widely used in many countries' construction industry due to their excellent structural performance. Traditionally, carbon steel tube is usually adopted in CFST columns. However, with the rising demand on the durability of structures, employing the stainless steel materials in the CFST structures as an alternative replacement for carbon steel is regarded as an effective method due to the fact that stainless steel is more durable and has great corrosion resistance (Tao *et al*. 2011).

To use concrete filled stainless steel tubular (CFSST) columns in a structure, there is a strong need to develop economical and reliable connections between CFSST columns and other connected components. Connections play the most important role in transferring applied structural loads and providing stability to the entire structure by linking principal structural elements.

Recently, some studies have been carried out to investigate the realistic behaviour of composite joints with CFST columns under fire condition. Wang and Davies (2003) carried out experimental study on fire behaviour of CFST column assemblies with

[1)] PhD Candidate
[2)] Associate Professor
[3)] Doctor

extended end plates. Ding and Wang (2009) tested 10 CFST columns connected to steel beams under the ISO 834 fire exposure condition, and the joint component temperatures were measured. Han *et al*. (2008) carried out 6 fire tests on reinforced concrete (RC) beam to CFST column joints under ISO 834 standard fire. Song *et al*. (2010) reported 3 tests on CFST column to steel beam joints in heating and cooling fire, and a finite element model was proposed to simulate the test results.

A literature review indicates that no research has been conducted on the fire performance of the hybrid stainless-carbon steel composite beam-column joints consisting of the carbon steel beam and stainless steel composite column. To fill this research gap, this paper will focus on investigating the temperature distribution of the hybrid joints in heating and cooling fire theoretically. Based on the research in this paper, mechanical analysis of this type of composite joints can be done in the future to consider both the heating and cooling stages of a fire.

2. FINITE ELEMENT ANALYSIS MODELLING

To analyse the mechanical performance of CFSST column to steel beam joints with bolted connections in heating and cooling fire, generally, heat transfer analysis has to be carried out before the mechanical analysis to provide the temperature distributions according to the fire conditions. Therefore, in this paper, a finite element (FE) model is developed by using ABAQUS software to simulate the temperature field of CFSST column to carbon steel beam joints. The joint is composed of one square CFSST column, two H-shaped carbon steel beams and one composite slab. Steel end plates are welded to the ends of the beams, and blind bolts are used to connect the beams to the steel tube. One row of shear connectors with uniform spacing of 200 mm are used to connect the composite slab to the steel top flanges.

2.1 Fire curve

Temperature distribution in the joint is directly influenced by the applied fire amplitude. A real fire event is characterised by three phases including growing phase, full-developed phase and decay phase. Due to changes in the amount of oxygen combustible material, prediction of growing fire is a difficult task, which is not an aspect covered in this paper.

To evaluate structural behaviour under fire conditions, commonly the standard fire curve proposed by ISO 834 (1980) is adopted by many researchers. In this research, the same fire curve in ISO 834 (1980) including heating and cooling phases, as shown in Fig. 1, is adopted. In this figure, T is the fire temperature in °C; t is the fire exposure time in minute; t_h is the heating time in minute; T_h is the fire temperature corresponding to t_h; t_p is the total fire exposure time in minute and T_o is the ambient temperature in °C, which is considered to be T_o = 20°C.

2.2 Material properties

Material thermal properties required in identifying development of temperatures in

structural members include thermal conductivity, specific heat and density. For concrete, the thermal properties proposed in Eurocode 2 (2005) part 1-2 are adopted in this paper, in which the thermal conductivity and specific heat capacity are temperature dependent. The concrete density is taken to be varied with temperature in accordance with Eurocode 2 (2005) part 1-2, and the concrete moisture content is taken as 5%.

The thermal conductivity and specific heat of carbon steel are taken from Eurocode 3 (2005) part 1-2, and the steel density is considered to be independent of the temperature and equals to 7850 kg/m^3. For the stainless steel, thermal conductivity and specific heat models given in Eurocode 3 (2006) part 1-4 are used in the current analysis, and the stainless steel density is 7850 kg/m^3.

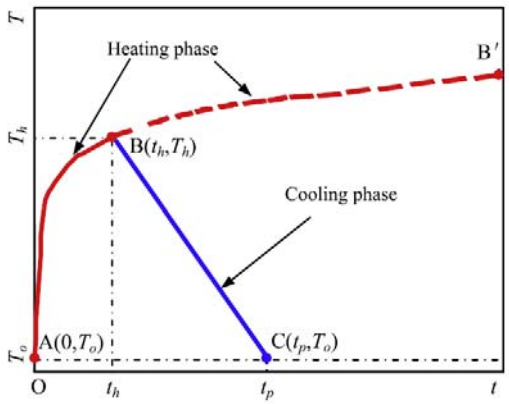

Fig. 1 Heating and cooling fire curve in ISO 834 (1980)

2.3 Boundary conditions

In the FE model, fire load is applied to the bottom parts of the joint below the composite slab, and the joint above the composite slab is exposed to the ambient temperature. The effects of heat convection and radiation are set as boundary conditions in the temperature field analysis.

During the heating phase of the fire, the heat flux transfers from fire environment to the composite joint, whereas in the cooling phase of the fire, the heat flux transfers from the composite joint to the environment. The initial ambient temperature before the application of the fire load is considered to be 20°C and is assigned as a predefined condition to the FE model. According to ECCS (1988), the boundary conditions can be set from Eq. (1).

$$-\lambda\left(\frac{\partial^2 T}{\partial x^2}+\frac{\partial^2 T}{\partial y^2}+\frac{\partial^2 T}{\partial z^2}\right)=\alpha\left(T-T_f\right)+\varepsilon\sigma[(T-T_z)^4-\left(T_f-T_z\right)^4] \quad (1)$$

in which, λ is the material thermal conductivity in W/(m K); T is the temperature at the point (x, y, z); α is the coefficient of convective heat transfer; T_f is the fire temperature which is time dependent as per ISO 834 (1980) standard fire curve; ε is the emissivity of surface; σ is the Stefan-Boltzmann constant with the value of 5.67×10^{-8} W/(m^2 K^4); and T_z is the absolute zero temperature equal to -273°C.

The value of coefficient of convective heat transfer for carbon steel is considered to be 25 W/m^{2}K as recommended in Eurocode 1 (2002) part 1-2. However, the value of emissivity used in steel temperature calculation called relative emissivity in the current version of Eurocode 3 part 1-2 (2005) has been changed from 0.5 to 0.7. An examination of the background documents shows that introducing the shadow factor and box value in the current version of Eurocode 3 is due to the different values of resultant emissivity recommended by the two versions of Eurocode 3 (Ding and Wang 2009).

A study by Franssen (2006) reveals that using the formula recommended by the current version of Eurocode 3 (2005) part 1-2 for I-sections leads to a smaller section size, whereas the temperature at required fire resistance time remains the same. This results in unsatisfactory load-bearing capacity of the section. While shadow effect for square and circular hollow tubes is not considerable, adopting a resultant emissivity of 0.7 is accurately acceptable for CFST columns. In this paper, a resultant emissivity of 0.5 is considered for all fire exposed surfaces except the surface of the CFST column.

In Eurocode 3 (2005), a convective heat transfer coefficient (α) of 25 W/m^{2}K and an emissivity coefficient (ε) of 0.4 are recommended for stainless steel. However, based on test data carried out on temperature development in structural stainless steel sections, modified values of 35 W/m^{2}K and 0.2 for convective heat transfer coefficient (α) and emissivity (ε) respectively, were proposed by Gardner *et al*. (2010) for stainless steel materials.

Due to either initial gap between the steel tube and concrete or difference between the concrete and steel thermal expansions, an air gap may be developed at the interface between the steel and concrete core in the fire condition. The air gap causes a delay in concrete temperature rise. To reflect the heat resistance in the interface between the concrete and steel due to the developed air gap, a simplified model proposed by Tao and Gannam (2012) as shown in Eq. (2) is adopted.

$$h_j = a \cdot (l_c / 100)^{-b} \tag{2}$$

in which h_j is the thermal contact conductance in W/m^{2}K; l_c is the diameter of a circular tube or the side length of a square or rectangular tube in mm; a and b are constants of 516 and 2.373 for circular columns, and 115 and 0.85 for rectangular columns, respectively. If the cross-sectional size is over 300 mm, h_j is simply taken as 38.1 and 45.2 W/m^{2}K for circular and rectangular columns, respectively (Tao and Ghannam 2012).

2.4 Element divisions

In the FE model, the concrete in the column, steel tube, concrete slab, end plates, blind bolts and shear connectors are modelled using 8-node brick elements (DC3D8). The profile steel sheet is modelled using 4-node shell elements (DS4), and the steel bars in the slab are modelled by 2-node truss elements (DC1D2). The maximum element dimension is considered to be less than 12 mm. The actual blind bolts are not modelled exactly but replaced by cone-shaped blocks that are tied to the surface of connected members. Welds between the steel beam and end plate are not modelled. Instead, welded components are tied together to allow temperature transfer between

the connected components. All of the parts inside the concrete, including blind-bolts and slab reinforcement, are embedded in the concrete by using embedded constraint. Typical element meshes and parts configurations for the CFSST column to steel beam joint are presented in Fig. 2.

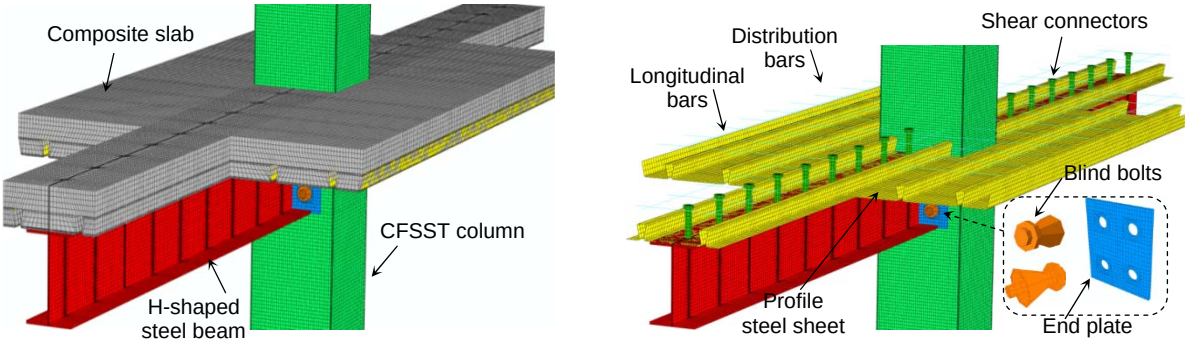

Fig. 2 Element meshing of the CFSST column to steel beam joint

3. Verification of the FE model

Due to the lack of test data of hybrid stainless-carbon steel beam-column joints subjected to heating and cooling fire, three types of temperature test data, including CFST column to steel beam joints in heating fire (Ding and Wang 2009), steel column to steel beam joints in heating fire (Dai *et al*. 2007) and CFST column to steel beam joints under heating and cooling fire (Song *et al*. 2010), are used to verify the established model.

3.1 CFST column to steel beam joints in heating fire

Experimental analysis of temperatures in different unprotected CFST column to steel beam joints was performed by Ding and Wang (2009). Five types of connections, including fin plate, web cleat, flush endplate, flexible endplate and extended endplate connections, were adopted in the joint specimens. Reinforced concrete slabs were not provided. But their effect on the temperature development was considered by using fire protection material (ceramic fibre blanket) to wrap the beam top flanges. The ISO 834 (1980) heating fire curve was adopted in the tests.

Among different joints investigated, extended endplate joints are considered in the verification study in this paper. Fig. 3 shows the comparisons between the tested and predicted temperature (T) versus time (t) curves corresponding to difference temperature measuring points, including points located at the top flange and web of the steel beam mid-section, end plate and bolt. The measuring points are marked on the sections by circles and crosses shown in Fig. 3. It can be seen that the FE model can predict the test results very well.

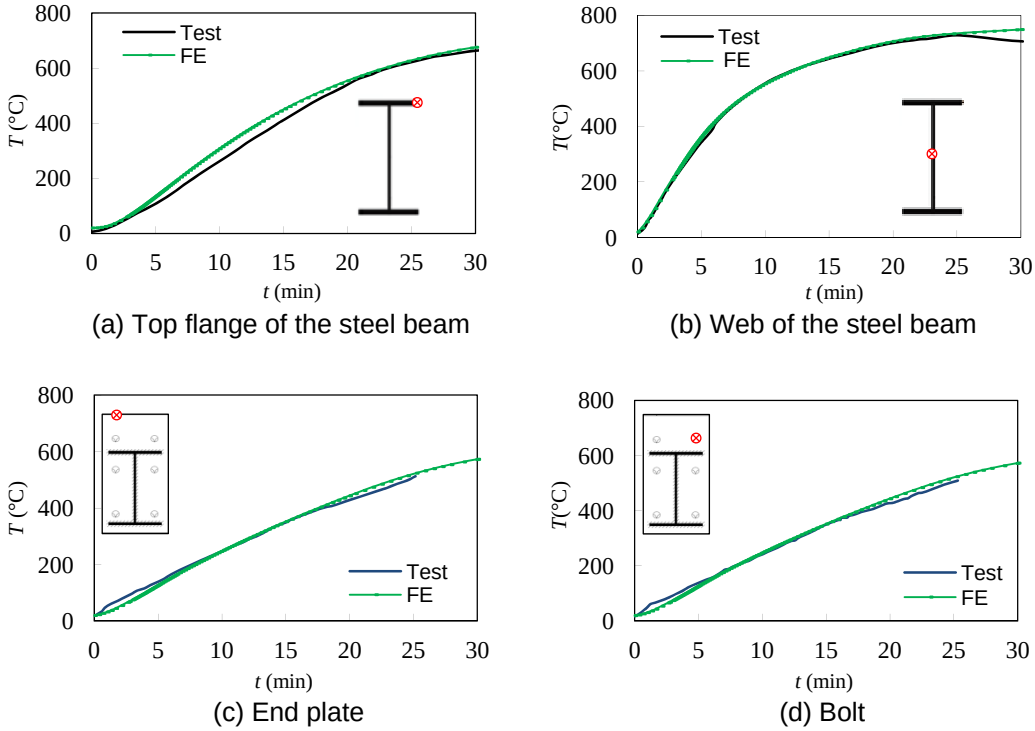

(a) Top flange of the steel beam (b) Web of the steel beam

(c) End plate (d) Bolt

Fig. 3 Tested and predicted temperature (T) versus time (t) curves of a CFST column to steel beam joint (tests 6 and 7 with extended end plates) in heating fire

3.2 Steel column to steel beam joints in heating fire

Dai *et al*. (2007) reported temperature test results of steel column to steel beam joints with composite slabs subjected to ISO 834 (1980) heating fire. Each joint specimen consisted of two beams connected to the steel column via fin plate connection. Fig. 4 shows some of the comparisons between the tested and predicted temperature (T) versus time (t) curves for a steel column to steel beam joint, and the predicted results agree well with the test results.

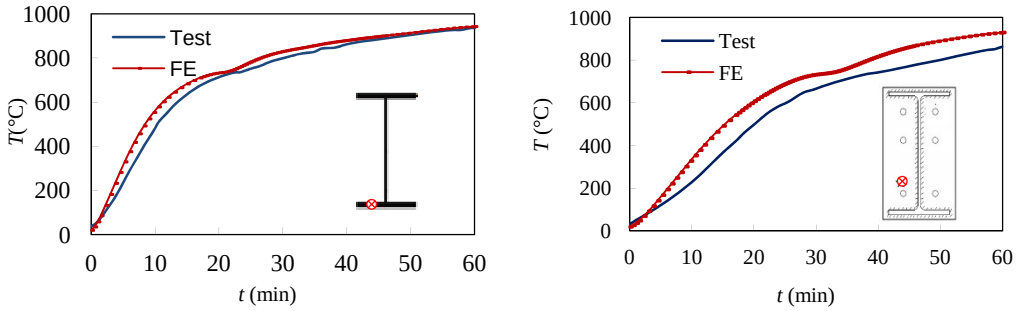

(a) Bottom flange of the steel beam (b) End plate

Fig. 4 Tested and predicted temperature (T) versus time (t) curves of a steel column to steel beam joint with flush end plates in heating fire

3.3 CFST column to steel beam joints in heating and cooling fire

Song *et al*. (2010) carried out experimental and theoretical research on three CFST column to steel beam joints with RC slabs subjected to the heating and cooling fire. The temperature distributions of the composite joints were measured during the tests, and a FE model was built to simulate the temperature development. Based on the proposed FE model in this paper, the temperature (*T*) versus time (*t*) curves of CFST column to steel beam joints in heating and cooling fire were predicted as shown in Fig. 5. Compared with the FE analysis in the original study, the following modifications are considered in the current FE model:

(1) Resultant emissivity of 0.5 for the beams, end plates and bolts and 0.7 for the column are adopted in the current FE model. A value of 0.5 was used for all components in the model proposed by Song *et al*. (2010).

(2) To reflect the heat resistance in the interface between the steel tube and concrete core, a simplified model proposed by Tao and Gannam (2012) is adopted in the current FE model, as described before. Instead, Song *et al*. (2010) ignored the heat resistance between the steel tube and concrete core.

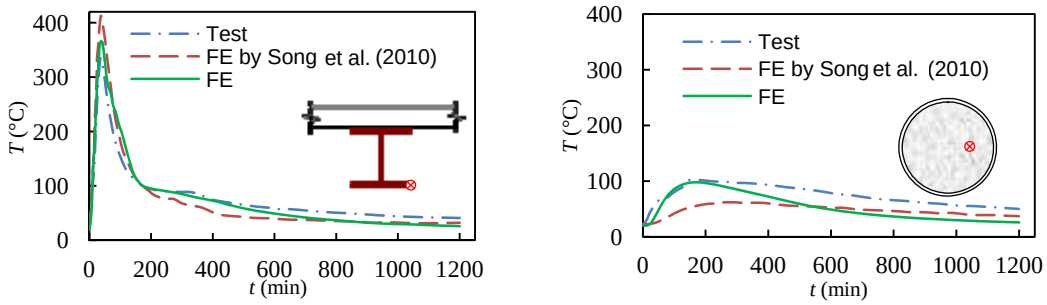

(a) Bottom flange of the steel beam (b) Concrete core of the CFST column

Fig. 5 Tested and predicted temperature (*T*) versus time (*t*) curves of a CFST column to steel beam joint (specimen JCFST2) in heating and cooling fire

Fig. 5 shows the comparison between the measured *T*-*t* curves, predicted curves by Song *et al*. (2010) and current predicted results corresponding to points at the bottom flange of the steel beam and in the concrete core of the CFST column in the panel zone. The preceding modifications considerably improve the predictions in the heating phase. The current predicted curves in the cooling phase are less accurate. Further research is required to investigate the thermal properties of materials in the cooling phase.

4. Temperature development analysis

Based on the verified FE model, the temperature distribution of a CFSST column to steel beam joint with a composite slab in heating and cooling fire is calculated and analysed. The results are compared with those of the joint with a carbon steel

composite column. For simplicity, joints with CFSST and CFST columns are referred to as CFSST and CFST joints in the following, respectively.

4.1 Calculation conditions

A cruciform beam-column joint isolated from a planar frame is chosen for the temperature development analysis, as shown in Fig. 6. The height of the CFSST column is 3800 mm. The width and thickness of the square stainless steel tube are 300 and 5 mm, respectively. The length of the H-shaped steel beam is 3900 mm. The height and width of the cross section of the steel beam are 252 mm and 146 mm, respectively. The thickness of the web and flanges of the steel beam are 6.1 mm and 8.6 mm, respectively. The thickness of the composite slab is 120 mm, and the width and length are 1200 mm and 2000 mm, respectively. Other details of the CFSST joint are shown in Fig. 6, where BN and CN represent the beam and column sections at a distance 500 mm away from the column face or the bottom flange of the beam, respectively; and BJ and CJ represent the beam and column sections near the column face or in the panel zone, respectively.

The ISO 834 (1980) heating and cooling fire, as shown in Fig. 1, is applied on the parts of the composite joint below the composite slab. The heating time (t_h) is taken as 30 min. For the CFST joint, the same dimensions as these of the CFSST joint are adopted except that the stainless steel tube is replaced by a carbon steel tube.

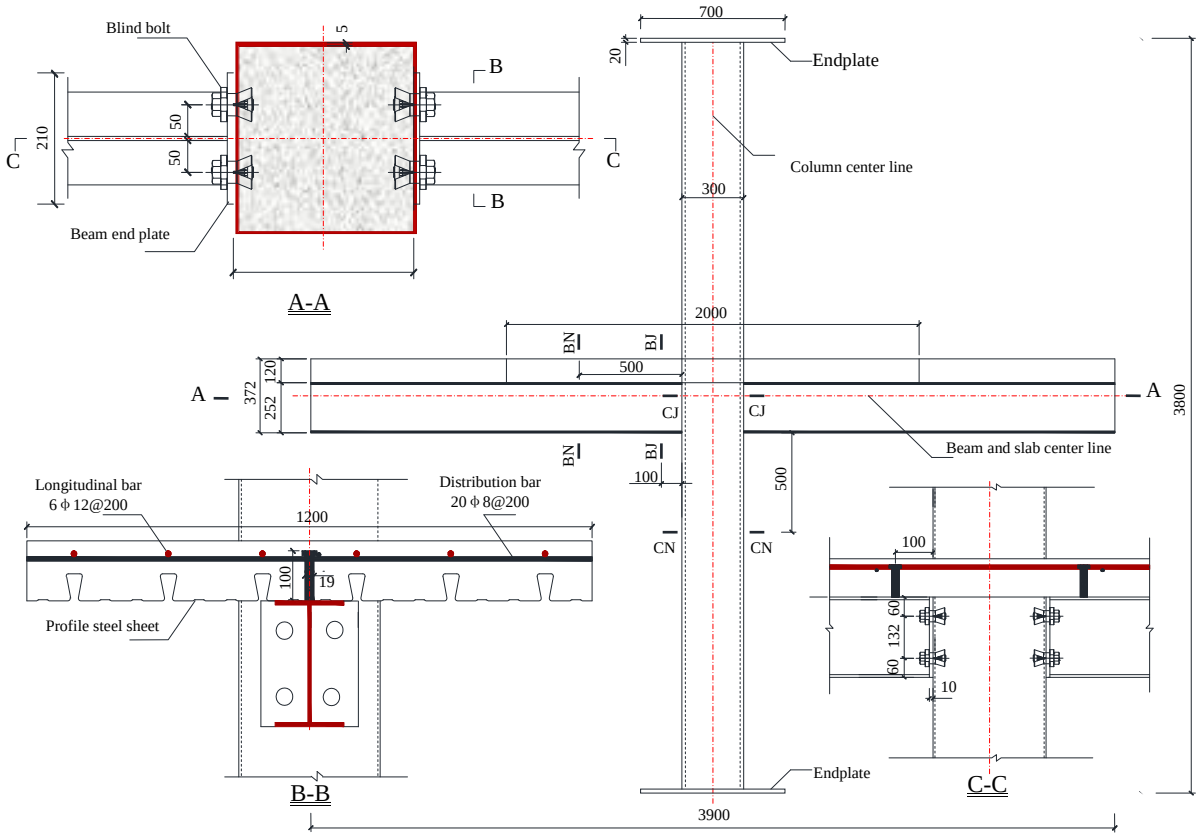

Fig. 6 Dimensions of the CFST column to steel beam joint (Unit: mm)

4.2 Temperature distributions in the beam and slab

Due to the short heating time of 30 min, the temperature distribution of the beam and slab away from the panel zone is quite close to that of the section close to the panel zone. If stainless steel is used, the beam temperature of section BJ may be slightly lower. However, due to good thermal conductivity of the steel the steel type of the column has inconsiderable influence on the temperature distribution of the beam and slab. This influence is more obvious for the points inside the concrete slab. Fig. 7 shows the temperature (*T*) versus time (*t*) curves corresponding to different points in section BJ (see Fig. 6) during the heating and cooling fire. The following observations can be made:

(1) A highest temperature of about 810° C can be observed in the bottom flange of the beam. Due to the excellent thermal conductivity of steel, there is not considerable temperature difference between the point on the bottom flange and the point on the web of the beam.

(2) The maximum temperatures of 660°C, 570°C and 300°C are obtained for the points on the top flange of the beam, on the profile steel sheet and inside the concrete slab respectively. It can be observed from the results that due to the heat absorption (heat sink effect) by the slab, a significant temperature difference appears between the bottom flange of the beam and the concrete slab. The temperature difference between the top and bottom flanges of the beam is about 150°C, but that between Point 5 inside the slab and Point 1 on the bottom flange of the beam reaches 510°C. The temperature of the inside concrete keeps increasing in the beginning of the cooling phase. At a *t* of 100 min in the cooling stage, the temperatures inside the concrete slab are higher than those of the steel beam. At this moment, the maximum slab temperature is 170°C.

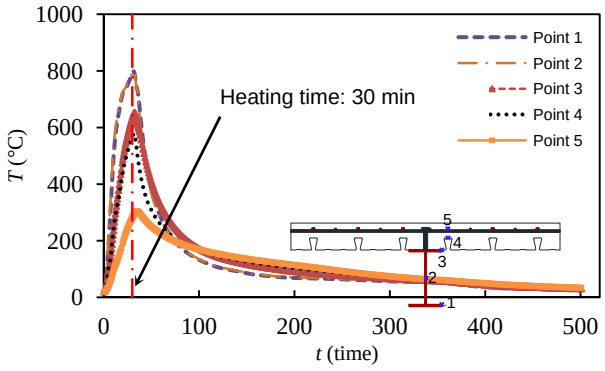

Fig. 7 Temperature (*T*) versus time (*t*) curves for different locations in the beam section BJ near the panel zone

4.3 Temperature distributions in the column

Fig. 8 shows the maximum temperatures at different points in the column sections CJ and CN for both CFSST and CFST joints. The following observations can be made:

(1) For the steel tube of Section CN, the maximum temperatures at Point 1 are 630°C and 710°C for stainless steel and carbon steel, respectively. The temperature difference indicates possible improved fire performance for the CFSST column in comparison to the CFST column. But for the steel tube in the panel zone, the temperature difference between the CFSST and CFST columns is minor, as shown in Fig. 8(a).

(2) For the inner part of the concrete core, the temperature at a location keeps increasing for a considerably long time after the commencement of the cooling phase and reaches its maximum value at a later stage. For Section CN of the CFST column, the maximum temperature of 188°C is obtained at Point 5 after 20 min from the beginning of the cooling phase. Similarly, at the same location of CFSST column, the maximum temperature is 150°C, which occurs after 34 min from the beginning of the cooling phase. The concrete core heats up with a lower rate in the CFSST column.

(3) For CFST columns, the temperature at Point 1 in the panel zone is lower than that at the same location (Point 6) away from the panel zone. This has been well-documented by many researchers due to the fact that the adjacent components in the panel joint absorb part of the heat that should be transferred to Point 1. But for CFSST columns, the trend is on the opposite. This may be attributable to the fact that additional heat is transferred from the carbon steel beam to the stainless steel column.

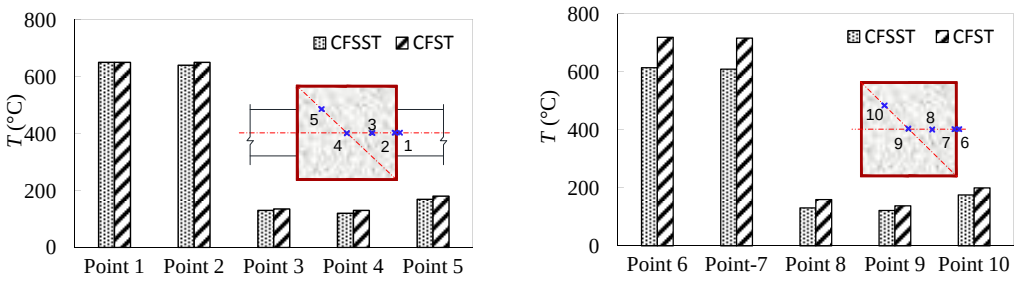

(a) Column section CJ in the panel zone (b) Column section CN

Fig. 8 Maximum temperatures of different points in CFSST and CFST columns

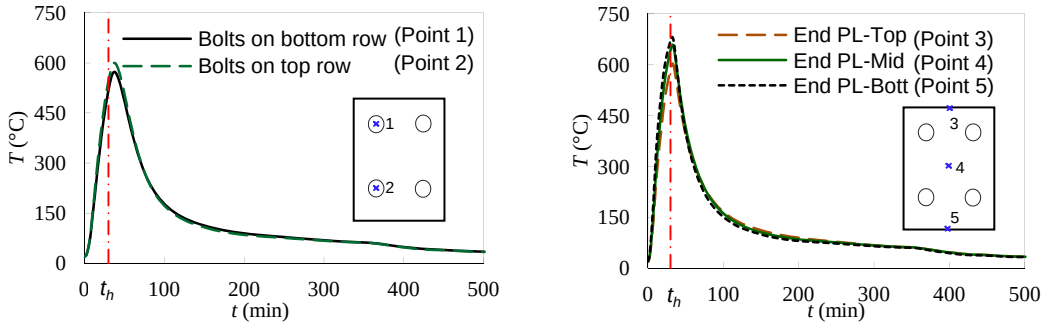

(a) Blind bolt (b) End plate

Fig. 9 Temperature (T) versus time (t) curves for the end plate and blind bolts in the CFSST joint

4.4 Temperature distributions in the bolts and end plates

The temperature distributions for the end plates and bolts in CFSST and CFST joints are observed to be similar. Thus only the FE results of the CFSST joint will be presented in this section. Fig. 9 shows the temperature (*T*) versus time (*t*) curves in the bolts on the top and bottom rows and those at different positions of the end plate.

Fig. 9(a) indicates that the *T-t* curves of the bottom and top bolts are nearly the same. The blind bolts are embedded in the concrete, and their temperatures are affected more by the concrete core compared a normal bolt. The temperature of the embedded part of a blind bolt is lower. Future research is required to check the potential beneficial influence.

Fig. 9(b) shows that the temperature at Point 3 on the top of the end plate, which is near the concrete slab, is slightly lower than that at other locations of the end plate. The maximum temperatures of 603°C and 680°C are obtained for Point 3 and Point 5, respectively. This is attributable to the heat sink effect of the slab.

5. Conclusions

The following conclusions can be drawn based on the current study:

(1) A FE model is established to simulate the temperature field of the CFSST column to carbon steel beam joint in heating and cooling fire. The influence of different resultant emissivity for different components and the heat resistance between the steel tube and concrete core are considered in the model.

(2) Beam and slab temperature distributions are not obviously affected by the steel material used in the column. For sections with different distances from the panel zone, the temperature distributions are almost similar. The influence of the steel type of the column is minor for the temperature distribution of the beam and slab.

(3) In terms of the temperature distribution in the column, some differences between the CFSST and CFST columns are observed. For the CFSST column, the temperature in the panel zone is higher than that at the same location away from the panel zone.

Acknowledgements

The research reported in the paper is part of the Discovery Project scheme (DP120100971) supported by the Australian Research Council (ARC). The financial support is gratefully acknowledged.

References

Dai, X., Wang, Y.C. and Bailey, C., (2007), “Temperature distribution in unprotected steel connections in fire”, *Proceedings of ‘3 International Conference on Steel and Composite Structures,* Manchester, UK, 535-540.

Ding, J. and Wang, Y.C. (2009), “Temperatures in unprotected joints between steel beams and concrete-filled tubular columns in fire”, *Fire Safety J*., **44**(1), 16-32.
ECCS-Technical Committee 3 (1988), *Fire safety of steel structures*, technical note: Calculation of the fire resistance of centrally loaded composite steel-concrete columns exposed to the standard fire.
Eurocode 1. BS EN 1991-1-2: 2002 (2002), *Actions on structures, Part 1-2*, *General actions – actions on structures exposed to fire.* British Standards Institution, London.
Eurocode 2. BS EN 1992-1-2:2004 (2005), *Design of concrete structures, Part 1-2, General rules−structural fire design*. British Standards Institution, London.
Eurocode 3. BS EN 1993-1-2:2001 (2005), *Design of steel structures, Part 1-2, General rules− structural fire design.* British Standards Institution, London.
Eurocode 3. BS EN 1993-1-4:2006 (2006), *Design of steel structures, part 1–4: General rules−supplementary rules for stainless steel*, British Standards Institution, London.
Franssen, J.M. (2006), “Calculation of temperature in fire-exposed bare steel structures: Comparison between ENV 1993-1-2 and EN 1993-1-2”, *Fire Safety J.*, **41**(2), 139-143.
Gardner, L., Insausti, A., Ng, K. and Ashraf, M. (2010), “Elevated temperature material properties of stainless steel alloys”, *J. Constr. Steel. Res*., **66**(5), 634-647.
Han, L.H., Zheng Y.Q., Tao, Z. and Wang, W.H., (2008) “Experimental behaviour of reinforced concrete beam to concrete filled steel tubular column joints under fire”. *Proceedings of* ‘*10 International Symposium on Structural Engineering for Young Experts*, Changsha, China, 47-52.
ISO 834 (1980), *Fire-resistance tests-elements of building construction*, International Standard ISO 834: Amendment 1, Amendment 2.
Song, T.Y., Han, L.H. and Uy, B. (2010), “Performance of CFST column to steel beam joints subjected to simulated fire including the cooling phase”, *J. Constr. Steel. Res.,* **66**(4), 591-604.
Tao, Z. and Ghannam, M. (2012), “Refined FE model to predict the temperature field within concrete-filled steel tubes”, *Proceedings of Seventh International Conference on Advances in Steel Structures,* Nanjing, China, 781-789.
Tao, Z., Uy, B., Liao, F.Y. and Han, L.H. (2011), “Nonlinear analysis of concrete-filled square stainless steel stub columns under axial compression”, *J. Constr. Steel. Res*., **67**(11), 1719-1732.
Wang, Y.C. and Davies, J.M. (2003), “An experimental study of the fire performance of non-sway loaded concrete-filled steel tubular column assemblies with extended end plate connections”, *J. Constr. Steel. Res*., **59**(7), 819-838.